Feature Article:

DOI. No. 10.1109/MAES.2017.160113

Complementary Pair Radar Waveforms—Evaluating and Mitigating Some Drawbacks

***Nadav Levanon, Itzik Cohen, Pavel Itkin*, Tel Aviv University, Tel Aviv, Israel**

INTRODUCTION

Complementary pulse pair is a radar waveform that achieves the ultimate range sidelobe reduction zero sidelobe. It is an early and simple embodiment of radar waveform diversity (WD), presently a popular topic. However, the use of complementary pulse waveforms is not widely spread because of several drawbacks. The main problem is the sensitivity to Doppler shift. Usually the two complementary coded pulses are separated in time. Doppler shift causes a phase ramp as function of time. That ramp causes two problems: (a) the two pulses in a pair are centered on different average phases; (b) there is a phase ramp during each pulse. Problem (a) also known as slow-time mismatch, is handled by the pulse-to-pulse conventional Doppler processing, which provides slow-time phase compensation. Problem (b) requires fast-time compensation, not provided by a simple linear Doppler processor. It causes loss of the ideal delay-sidelobe cancellation resulting in near range-sidelobes. Those near sidelobes increase with longer codes and with higher Doppler shifts. At the same time a complementary pulse pair also causes a difficulty at low Doppler shifts.

Moving target indication (MTI) is a radar processing approach designed to help stationary pulse-Doppler radars to separate weak reflections of moving targets from strong returns of stationary clutter. This task becomes more difficult at low Doppler (slow targets). A classical MTI processor is constructed from a pulse canceller followed by discrete Fourier transform (DFT). A pulse canceller subtracts returns from consecutive pulses, assuming stationary clutter returns are identical and will cancel out. This concept fails if consecutive pulses are differently coded.

A very early version of MTI was used in the FPS-18 radar [1]. The receiver included a 3-pulse canceller followed by 8-pulse DFT. The interpulse weighting was a raised cosine. Special measures were added to circumvent the excessive attenuation of returns from very low-Doppler targets, caused by the three-pulse canceller.

Progress in devices and signal processing [2,3] allows considerable improvements in: (a) Doppler resolution (e.g., by increasing the coherent processing interval (CPI) by increasing the number of pulses in the CPI, while maintaining the pulse repetition interval (PRI); (b) range resolution (e.g., by pulse compression); (c) Doppler sidelobe reduction (e.g., by improved weighting windows); and (d) range sidelobe reduction (e.g., by using mismatched filters).

Since complementary pairs are phase-coded they suffer from high- and slow-decaying spectral sidelobes. There are several measures [4, sec. 6.8] to improve spectral efficiency of phase-coded waveforms. When applied to complementary pairs they raise the question of how well the zero range-sidelobes property is preserved.

This article considers the above issues, suggests mitigating measures, and evaluates performances. The specific complementary Golay binary pair in this demonstration is the longest ($L = 26$ element) known binary sequence pair [5] that is not constructed from shorter sequences. The phases of the pair are given by

$$\phi_1 = \pi\left[00011000101101010110010000\right]$$
$$\phi_2 = \pi\left[00001001101000001011100111\right]$$

The autocorrelation functions (ACF) of each coded pulse by itself are shown in subplots (a) and (b) of Figure 1. Note the equal magnitudes but opposite polarities at each delay, except at the origin. That fact is responsible for the sidelobes cancellation when the sidelobes of the two correlations are added. Such addition happens when a train of repeated complementary pulse pairs $\{s_1\, s_2\, s_1\, s_2\, s_1\, s_2\, s_1\, s_2 \ldots\}$ is cross-correlated with at least one reference pair. The resulting periodic cross-correlation, with a reference containing one complementary pulse pair $\{s_1\, s_2\}$, is shown in subplot (c) of Figure 1. Selected duty cycle of $d = 0.2$ resulted in a PRI five times longer than the pulse duration, namely

$$T_r = t_p/d = Lt_b/d = 26t_b/0.2 = 130t_b$$

where t_b is the duration of a code element (bit), L is the code length, t_p is the pulse duration, and T_r is the PRI.

The main property of a complementary pair is demonstrated in Figure 1(c) by the zero near-sidelobes at $1 \le |\tau/t_b| \le L = 26$. When the delay equals the PRI, signal and reference pulses overlap again but now the overlapping pulses are not matched. Signal pulse 1 is aligned with reference pulse 2 and signal pulse 2 overlaps reference pulse 1. This results in the recurrent delay lobes at the delay spans

$$\left(T_r - t_p\right)/t_b = (130 - 26) < |\tau/t_b| < (130 + 26) = \left(T_r + t_p\right)/t_b$$

Authors' current address: Dept. of Electrical Engineering–Systems, Tel Aviv University, Tel Aviv 6997801, Israel. E-mail: (nadav@eng.tau.ac.il).

Manuscript received May 11, 2016, revised August 8, 2016, and ready for publication September 18, 2016.
Review handled by D. O'Hagan.
0885/8985/17/$26.00 © 2017 IEEE

Note from Figure 1(c) that for this particular complementary pair the peak sidelobe ratio of the recurrent delay lobes is $20\log_{10}(8/52) = -16.25$ dB.

Selecting a reference containing only one complementary pair, namely only N (= 2) pulses, was done to simplify the drawings. Such a short CPI (CPI = 2 T_r) yields insufficient Doppler resolution. When meaningful Doppler resolution is desired, N would usually be a large even number. As pointed out earlier in this introduction section, Doppler spoils the zero near-sidelobes property of complementary pairs waveform. How bad the degradation is, is the subject of the next section, which presents the delay-Doppler response (without a pulse canceller).

DELAY-DOPPLER RESPONSE WITHOUT PULSE CANCELLER

The signal used is a periodic train of N=64 pulses constructed from 32 identical complementary pairs with L =26 elements in each pulse. The element duration is t_b implying a pulse duration t_p = $26t_b$. In order to simplify the drawings the duty cycle is d = 0.2. This implies PRI (between individual pulses, not between pairs): T_r = $5t_p$ = $130t_b$. The weight window preceding the DFT was Dolph-Chebyshev with sidelobe level of -62 dB [in MATLAB terminology: chebwin(64,62)].

Figure 2 displays the delay-Doppler response of a matched filter processor without pulse canceller. The response is given in dB with a floor of -65 dB. The peak of the response, at the ori-

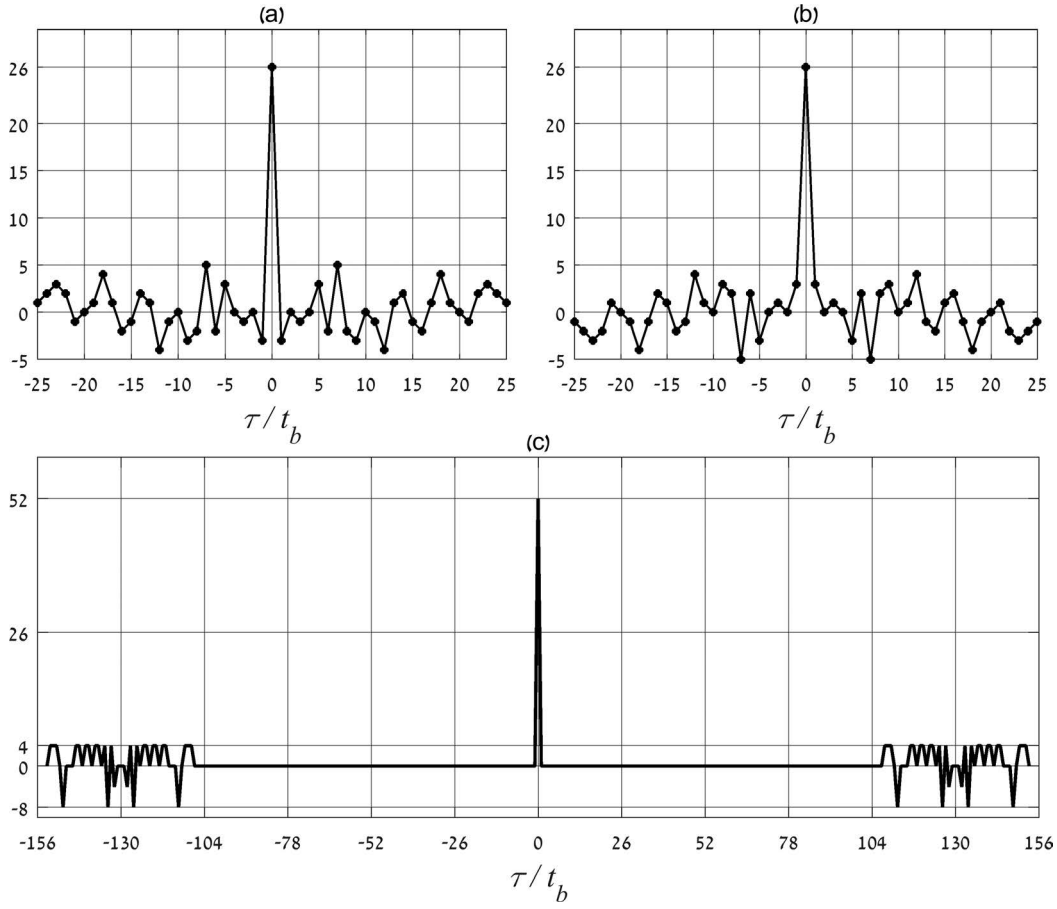

Figure 1.
(a) ACF of first coded pulse. (b) ACF of second coded pulse. (c) Periodic cross-correlation between the repeated pulse pair and a reference containing one pair.

gin, is -1.9 dB, reflecting loss due to the weight window. The delay τ axis is normalized by the code element duration t_b, in order to obtain dimensionless coordinates. For the same purpose the Doppler v axis is normalized by multiplying it by NT_r the duration of the CPI, (recall that $N = 64$). Thus, if NT_r is in seconds, v is in Hz. If NT_r is in milliseconds v is in kHz, etc. The observed response clearly shows no near sidelobes on the delay axis (zero-Doppler). Recurrent delay lobes appear around delay $\tau = T_r = 130t_b$, where one pulse of the transmitted complementary pair coincides with the wrong pulse of the reference complementary pair. The peak recurrent delay sidelobe (-18.19 dB) is 16.25 dB below the mainlobe (-1.933 dB), as found also in Figure 1(c). The sidelobe-free recurrent delay peak reappears at $\tau = 2T_r = 260t_b$, which is the effective periodicity of the signal ($=2T_r$).

A strong recurrent Doppler peak appears on the Doppler axis at $v = 1/T_r$, namely at $vNT_r = 64$. At this Doppler shift the Doppler induced phase ramp completes accumulating 2π between individual pulses. Near range-sidelobes appear around that recurrent peak and the peak value (= −2.5 dB) is only slightly lower than the peak at the origin (= −1.9 dB). Both are due to the sensitivity of complementary-pair waveform to Doppler. There is also a relatively weak recurrent Doppler ridge at $vNT_r = N/2 = 32$, namely at $v = 1/(2T_r)$. At that Doppler shift the Doppler induced phase ramp accumulates π between pulses, thus reversing polarity every pulse. This explains the null (hard to see) in that ridge on the Doppler axis. It is worth recalling that a lobe at any coordinate (τ_1, v_1) of the delay-Doppler response implies that a signal reflected with additional delay τ_1 and additional Doppler v_1 will be attributed to the nominal delay and Doppler (0,0). Along the Doppler axis ($\tau/t_b = 0$) we see the near-constant −62 dB sidelobes of the mainlobe at the origin, predicted by the chebwin(64,62) interpulse weight window.

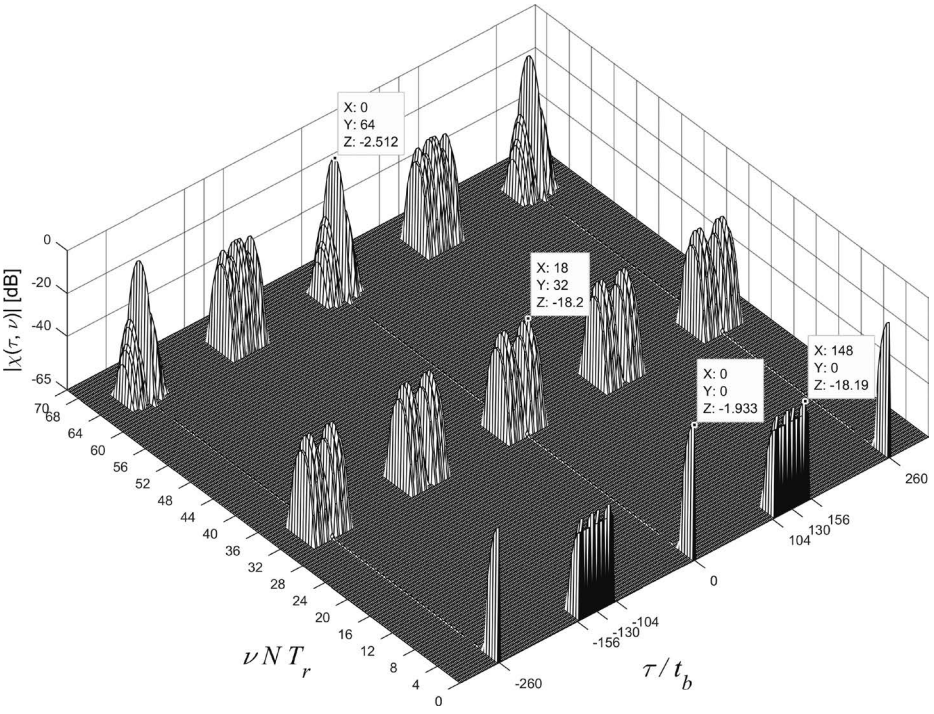

Figure 2.
Delay-Doppler response, $|\tau| \le 2T_r + t_p$.

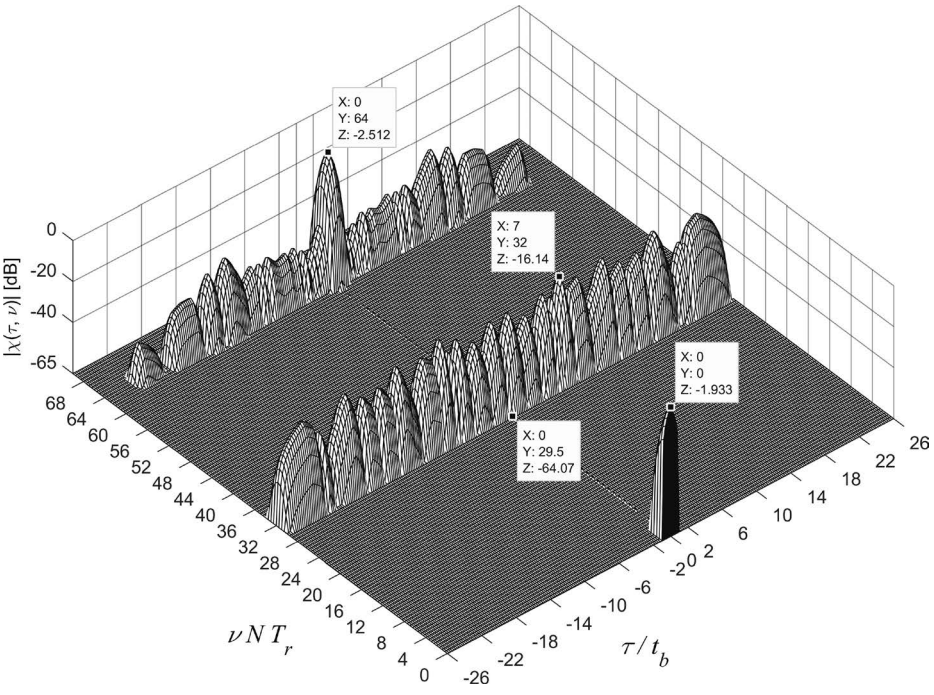

Figure 3.
Delay-Doppler response, Doppler shift = 0, no pulse canceller. Zoom on $|\tau| \le t_p$.

A zoom in delay of the same delay-Doppler response is shown in Figure 3. The zoom allows us to see clearly the width of the mainlobe at the origin. It is also easier to see the recurrent peak at $\tau/t_b = 0$, $vNT_r = 64$ compared with the null at $\tau/t_b = 0$, $vNT_r = 32$. (The corresponding data point was pulled slightly backward to $\tau/t_b = 0$, $vNT_r = 29.5$ to make it visible.)

Figure 4 (bottom) shows the phase ramp as function of time caused by Doppler shift. The top subplot shows the slow-time compensation provided by the DFT in a conventional pulse-Doppler processor. The intrapulse phase ramp is not compensated, which results in imperfect delay-sidelobe cancellation and a rise in the near-sidelobes at non-zero Doppler, as shown in Figure 5.

Figure 5 displays the delay-Doppler response at the output of a processor matched to a Doppler shift of $vNT_r = 4$. A weak buildup of the range near-sidelobes is seen, but no significant change is seen in the mainlobe height. The difference between the mainlobe and peak sidelobe (≈ 50 dB) is still acceptable. The range near-sidelobe will increase with increasing Doppler.

TWO-PULSE CANCELLER FOR COMPLEMENTARY-PAIR WAVEFORM

In coherent pulse train constructed from repeated pairs of complementary pulses, the delay used in a two-pulse canceller must be of length $p2T_r$, $p = 1,2,\ldots$. Only then the subtraction would be of returns from an identically coded pulses. The shortest delay is therefore $2T_r$. A block diagram of such a two-pulse canceller appears in Figure 6. The response of a 2-pulse canceller is shown in Figure 7. Log frequency scale was used because we wish to emphasize low Doppler frequencies. The top subplot of Figure 7 describes the response of a 2-pulse canceller when the delay is $2T_r$. The first null occurs at $v = 1/(2T_r) \rightarrow vNT_r = \mathrm{N}/2 = 32$. Recall that the frequency response of our 2-pulse canceller, whose delay equals $2T_r$, is given by (1), which explains the peak of 6 dB in the top subplot of Figure 7.

$$\left|H(v)\right| = 2\left|\sin\left(2\pi v T_r\right)\right| \rightarrow \max\ H(v)\Big| = 2 \tag{1}$$

The middle subplot shows the response of the fourth Doppler filter out of 64 DFT outputs. The peak level of -1.93 dB reflects the loss caused by the weight window. Cascading the two top responses will result in the bottom

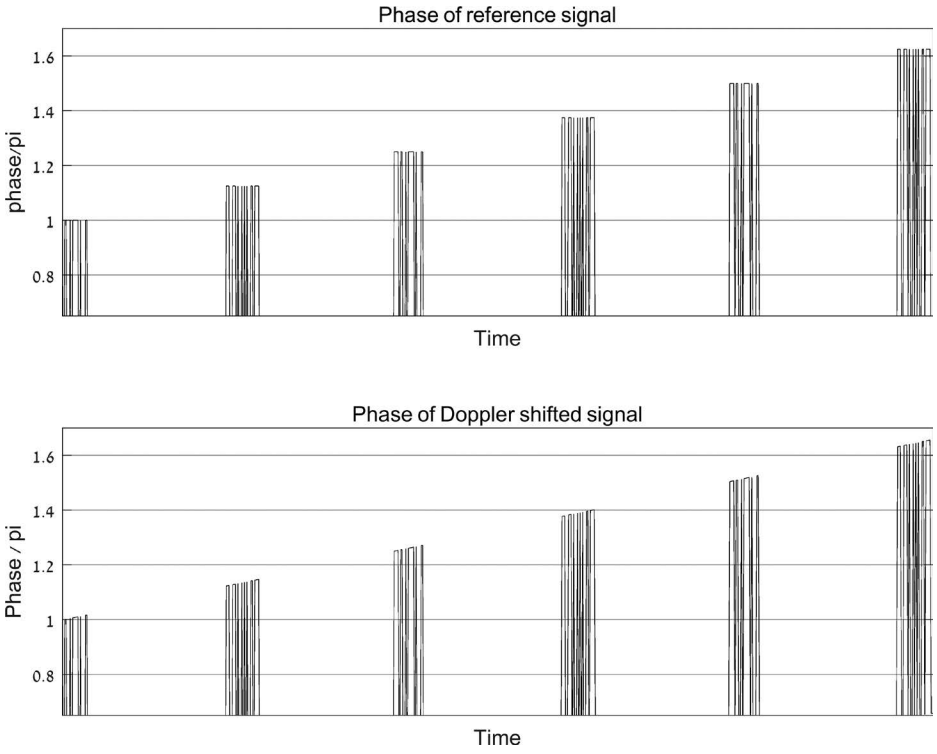

Figure 4.
Doppler induced phase ramp of the received complementary pulse train (bottom). Slow-time phase compensation provided by a conventional linear pulse-Doppler processor (top).

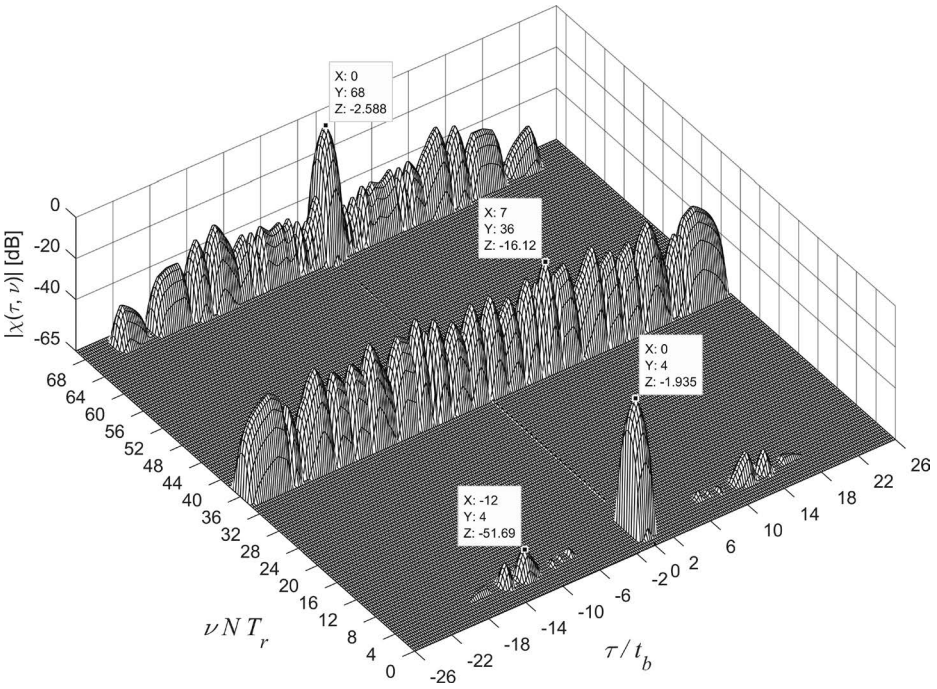

Figure 5.
Delay-Doppler response, Doppler shift $vNT_r = 4$, no pulse canceller. Zoom on $|\tau| \le t_p$.

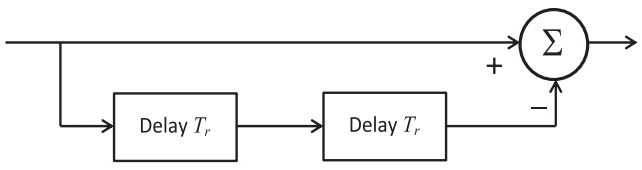

Figure 6.
The shortest two-pulse canceller for complementary pair pulse train.

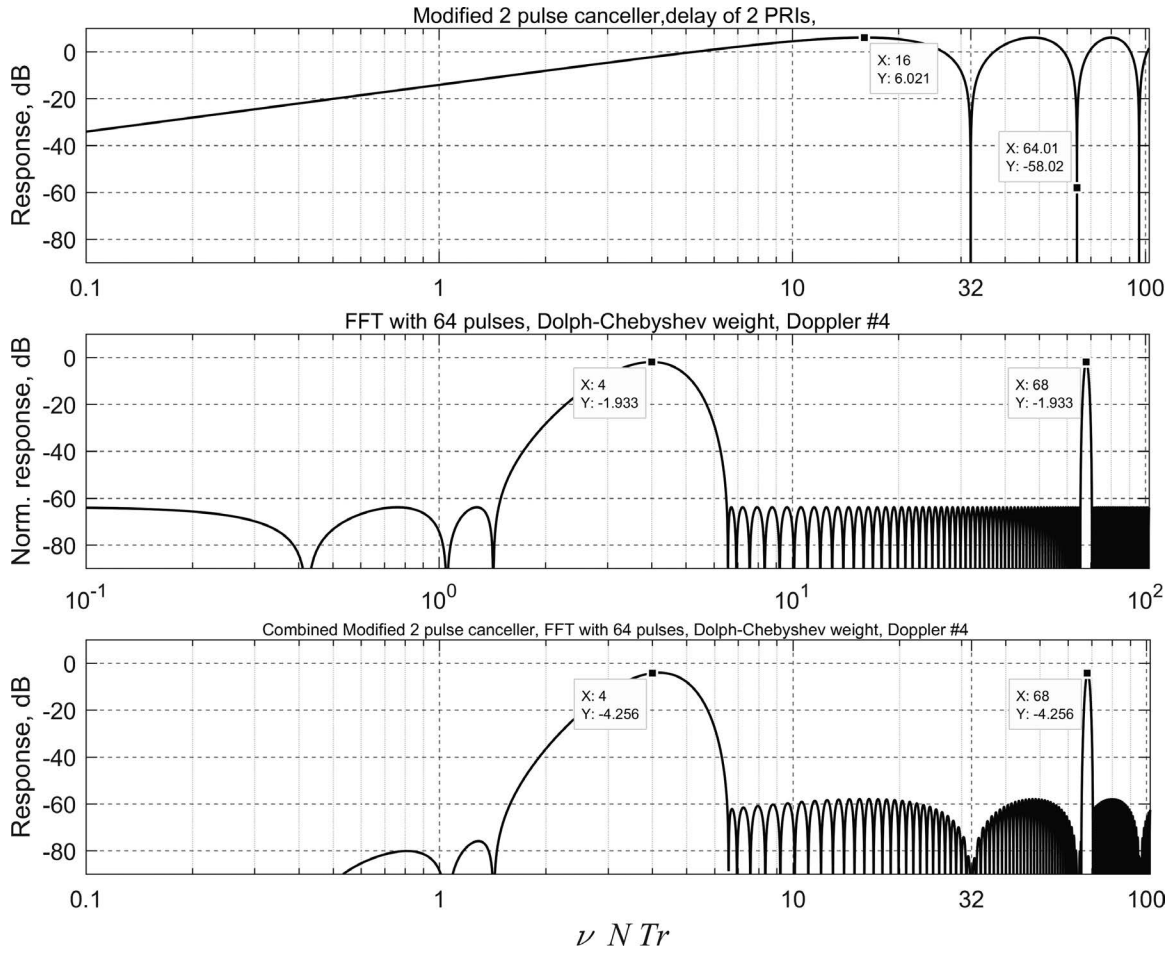

Figure 7.
The frequency response of the 2-pulse canceller (top), the weighted FFT (middle), and the combined response (bottom), for the fourth Doppler window.

subplot. It is the combined Doppler response at zero delay.

The responses in Figure 7 are Doppler frequency responses. To see the delay-Doppler response we need to add the 2-pulse canceller and recalculate Figure 4. The resulting delay-Doppler response is shown in Figure 8. The calculation used the actual complementary pulse pairs, making the periodicity $2T_r$ instead of T_r. That explains the additional Doppler ridge at $vNT_r = N/2 + 4 = 32 + 4 = 36$.

Note that the bottom subplot of Figure 7 is the $\tau/t_b = 0$ cut of Figure 8, using a log scale of the Doppler axis. Thus, Figure 8 contains much more information than Figure 7. The calculation that yielded Figures 7 and 8 was repeated for Doppler filter $vNT_r = 1$. The results appear in Figures 9 and 10. Note the considerably stronger attenuation by the canceller at that low Doppler shift.

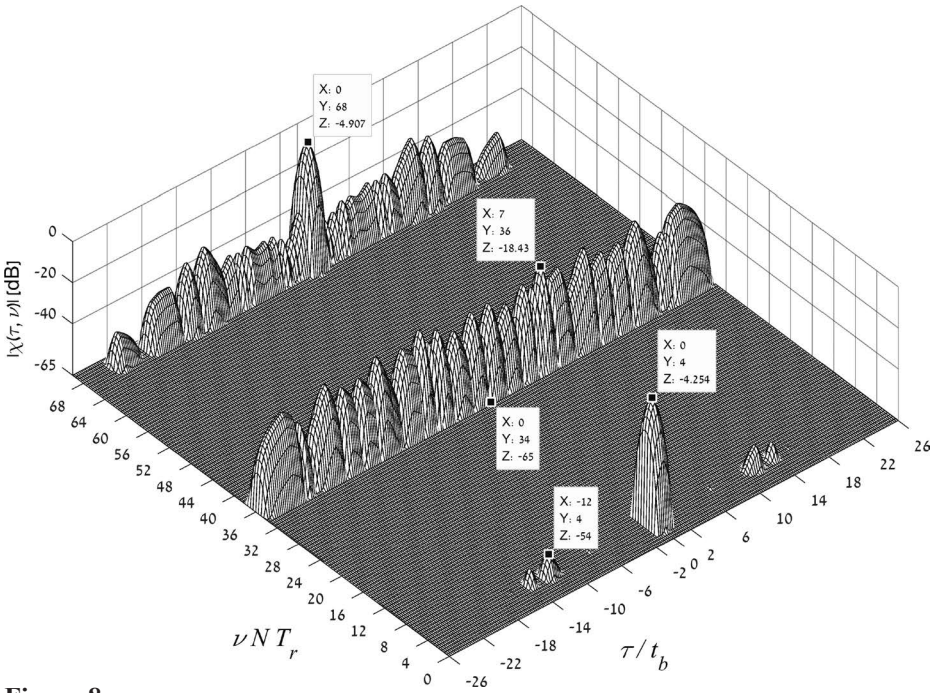

Figure 8.
Delay-Doppler response. Doppler shift $vNT_r = 4$, 2-pulse canceller, N=64. Zoom on $|\tau| \le t_p$.

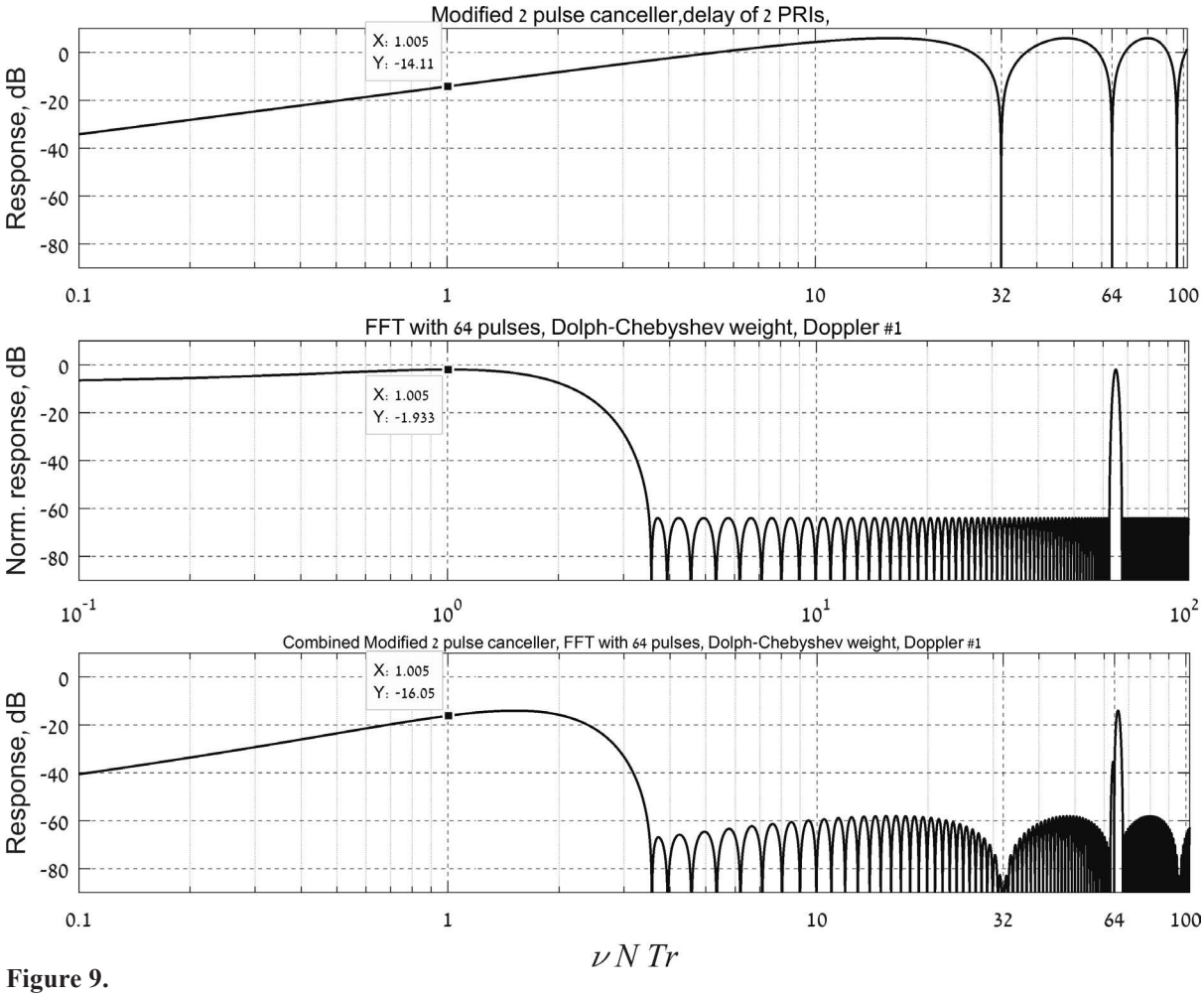

Figure 9.
The frequency response of the 2-pulse canceller (top), the weighted FFT (middle), and the combined response (bottom), for the first Doppler window.

REDUCING SPECTRAL SIDELOBES WHILE MAINTAINING CANCELLED RANGE SIDELOBES

We suggest a second version of the complementary waveform that exhibits more efficient spectrum, with reduced spectral sidelobes. In that version the rectangular shape of a bit is replaced by a "Gaussian windowed sinc" (GWS) [6], which extends over 4 bits,

$$GWS_m = \exp\left[-\frac{1}{2}\left(\frac{4m}{\sigma(4M+1)}\right)^2\right]\frac{\sin\alpha_m}{\alpha_m},$$
$$\alpha_m = \frac{4\pi m}{4M+1}, \quad m = -2M, -2M+1, ..., 2M \tag{2}$$

where M is the number of samples per code element (bit) and σ is a width parameter chosen as 0.7.

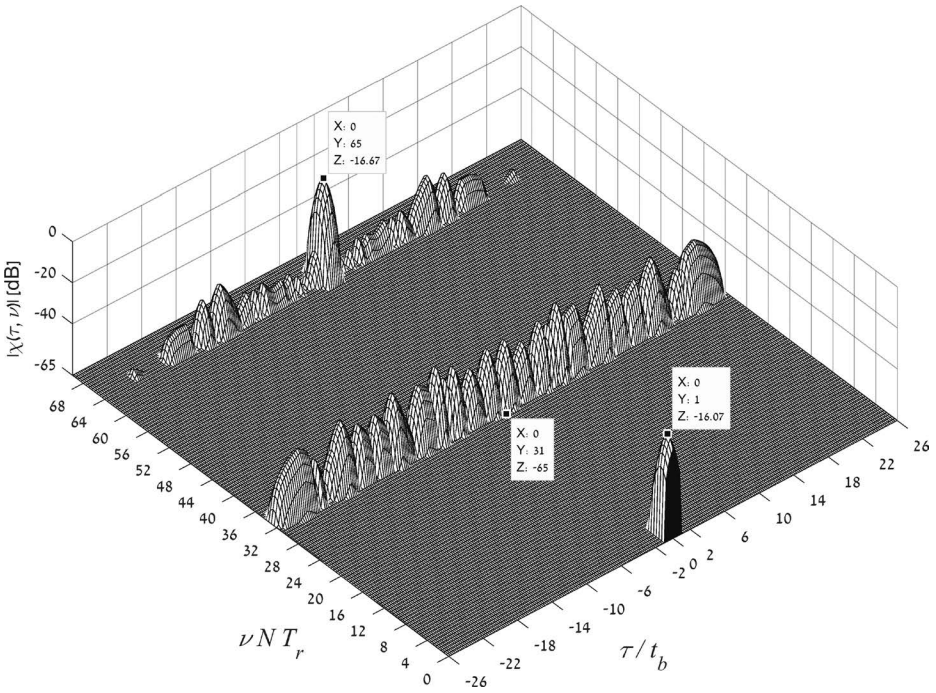

Figure 10.
Overall delay-Doppler response. Doppler shift $vNT_r = 1$, 2-pulse canceller, N=64. Zoom on $|\tau| \le t_p$.

Figure 11 shows the two complementary base-band signals using the rectangle shaped element (dash) and the GWS shaped element with $M = 4$ (solid). Since the GWS representation extends over 4 bits the duration of the GWS shaped complementary signal extends over 26+3 = 29 bits. In practice the transmitter and the receiver are likely to be bandwidth limited by the hardware, which will further modify the waveforms in Figure 11 as if they passed through a low-pass filter (LPF). It is therefore expected that the waveform in the upper subplots of Figures 11 and 12 will be smoothed as shown in the bottom subplot of Figure 12. Figure 13 shows the spectrum change between the original complementary signal, with rectangle element shape, and the 4 samples/bit GWS element shape after LPF. The LPF was a simple first order Butterworth filter with cutoff frequency $v_n = 5/t_b$.

We find it important to clarify that the LPF is not an intended part of the processing. It was added to represent a likely effect of the hardware's limited bandwidth. It is also important to point out that the waveform seen in Figure 12 (bottom) is the complex envelope of the signal, which happens to be real, that coherently modulates (in both amplitude and phase) a carrier frequency. Noncoherent amplitude modulation only will exclude Doppler processing and Doppler information.

The next obvious question is how the bandwidth reduction affected the autocorrelation and how well the zero range-sidelobe property was preserved. The answers are given in Figures 14 and 15. Figure 14 shows the periodic autocorrelation (linear scale) of the 26 element complementary pair when the element shape is 4 samples/element GWS, followed by LPF. Note that the only deviations from the ideal zero near-sidelobes

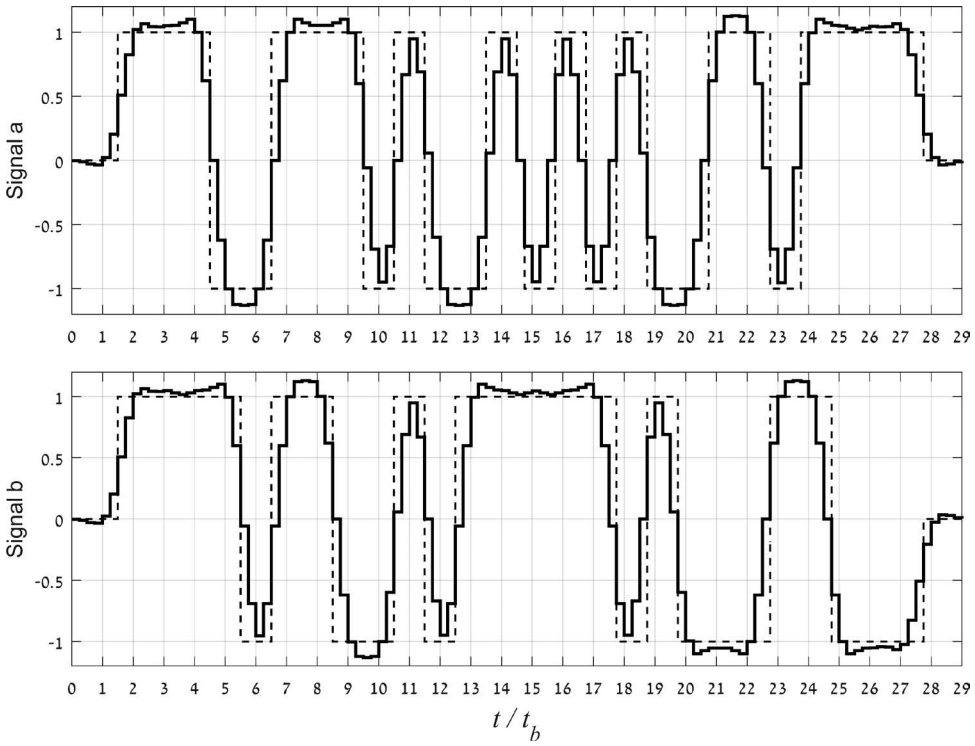

Figure 11.
The two complementary base-band waveforms, each with the two sequence element shapes: rectangle (dash), GWS with 4 samples per code element (solid).

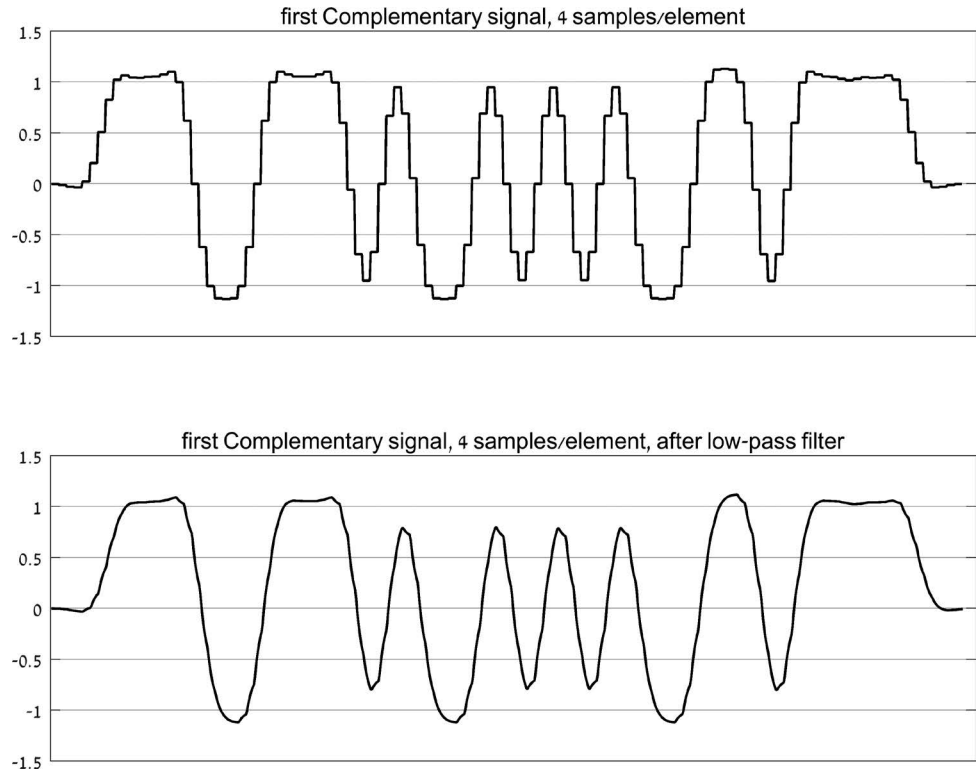

Figure 12.
The first complementary base-band waveforms with 4 samples/bit GWS, before (top) and after LPF (bottom).

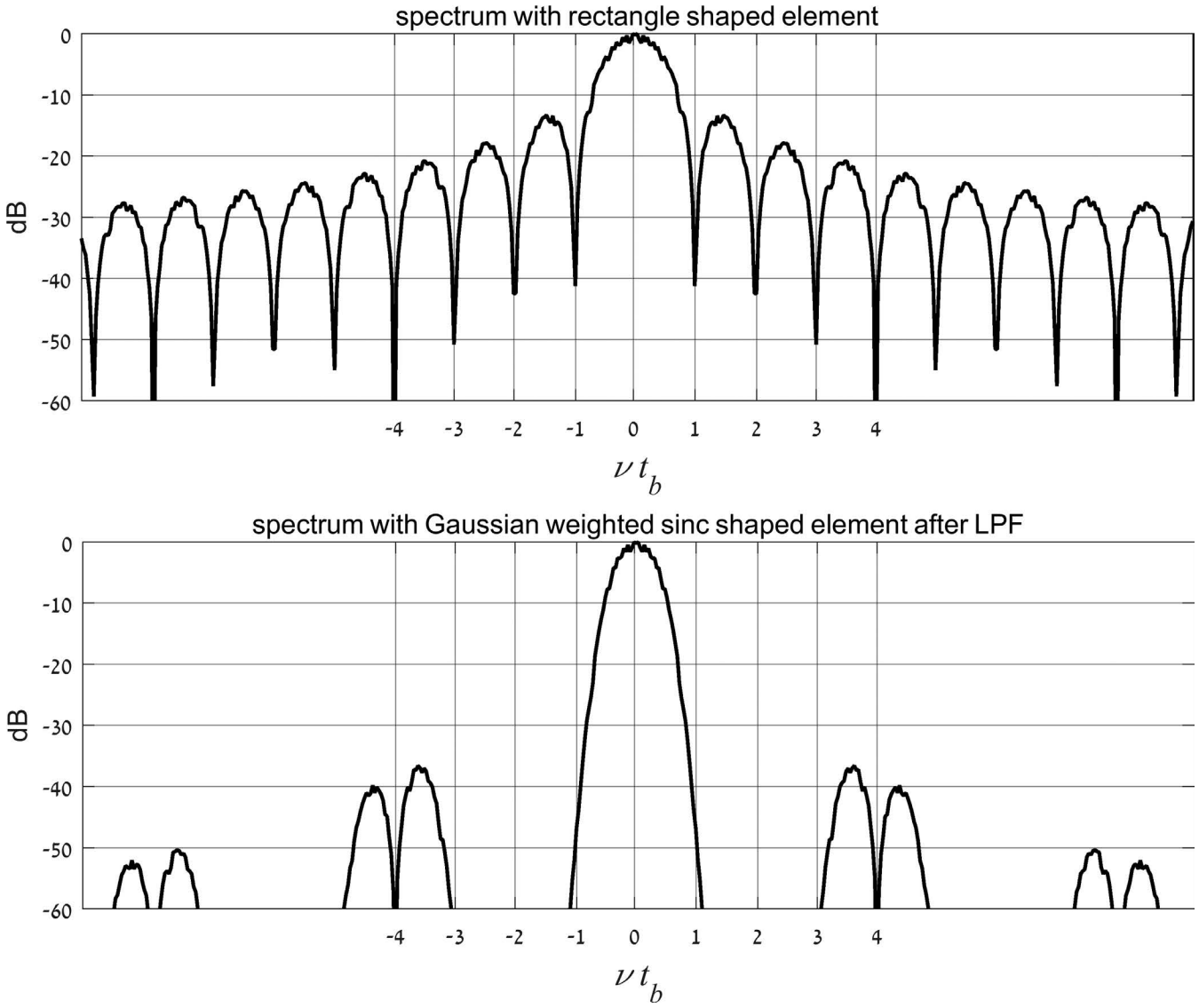

Figure 13.
Spectrums of the complementary base-band signal with rectangle element shape (top) and GWS shape followed by LPF (bottom).

response are the two small negative sidelobes on the immediate sides of the mainlobe. Their relative height is -34.7 dB. Figure 15 shows the corresponding delay-Doppler response (dB scale) with interpulse weight window chebwin(64,62). The response is normalized; hence the mainlobe peak value is 0 dB. Clearly marked is the immediate sidelobe on the delay axis, with a peak of -34.7 dB. The x = 62.5 reading on the data tip represents normalized delay of τ/t_b = 1.93. The value $x = -34.5$ on the next data tip implies $\tau/t_b = -1.07$.

CONSTANT AMPLITUDE WAVEFORMS

GWS representation of the phase-coded complementary pair reduced the spectral sidelobes and maintained the cancellation of the ACF near-sidelobes. The remaining drawback is the created variability in amplitude. An expected question is how well constant-amplitude, spectrally efficient conversions would maintain the

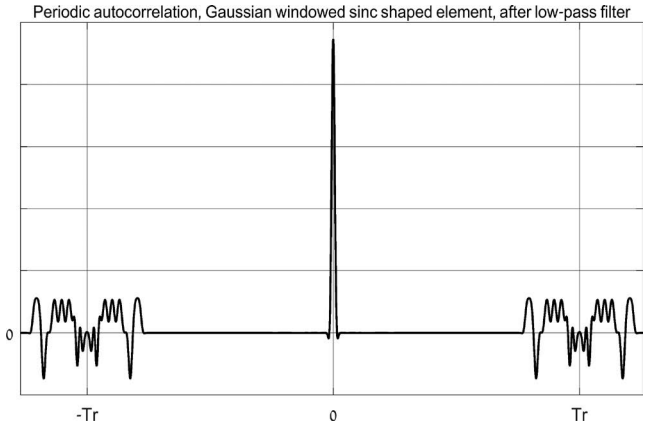

Figure 14.
Periodic autocorrelation of a 26 element complementary pair. Each element shape was created by 4 samples/element GWS followed by LPF.

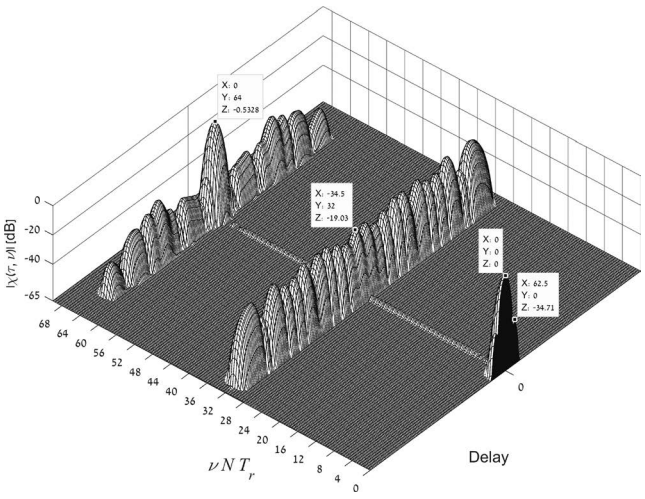

Figure 15.
Delay-Doppler response, GWS and LPF, Doppler shift = 0, no pulse canceller. Zoom on $|\tau| \le t_p$.

sidelobes cancellation. In [7] the originators of the GWS bit representation compared it with several constant-amplitude schemes (phase shift keying, minimum phase shift keying, and derivative phase shift keying) and found that those alternatives worsen the ACF sidelobes of coded radar waveforms. In [8] a continuous phase modulation (CPM) transformation was used, which also increased the delay sidelobes. A remedy described in [8] suggests using mismatched filters to reduce the sidelobes at a cost of some signal-to-noise ratio (SNR) loss. Such a remedy does not suit the concept of complementary pair sidelobe cancellation rather than sidelobe reduction.

Figure 16 compares the ACF mainlobe vicinity of the three spectrally efficient implementations. Only the GWS implementation (top) maintained the cancellation of the ACF near-sidelobes. In the CPM version (middle) high near-sidelobes reappear with a peak of −22 dB. The derivative-phase version (bottom) yielded peak near-sidelobe of −34 dB.

A fourth representation should be of interest. It uses the biphase-to-quadriphase transformation [9, 4 (sec. 6.8)]. The quad-

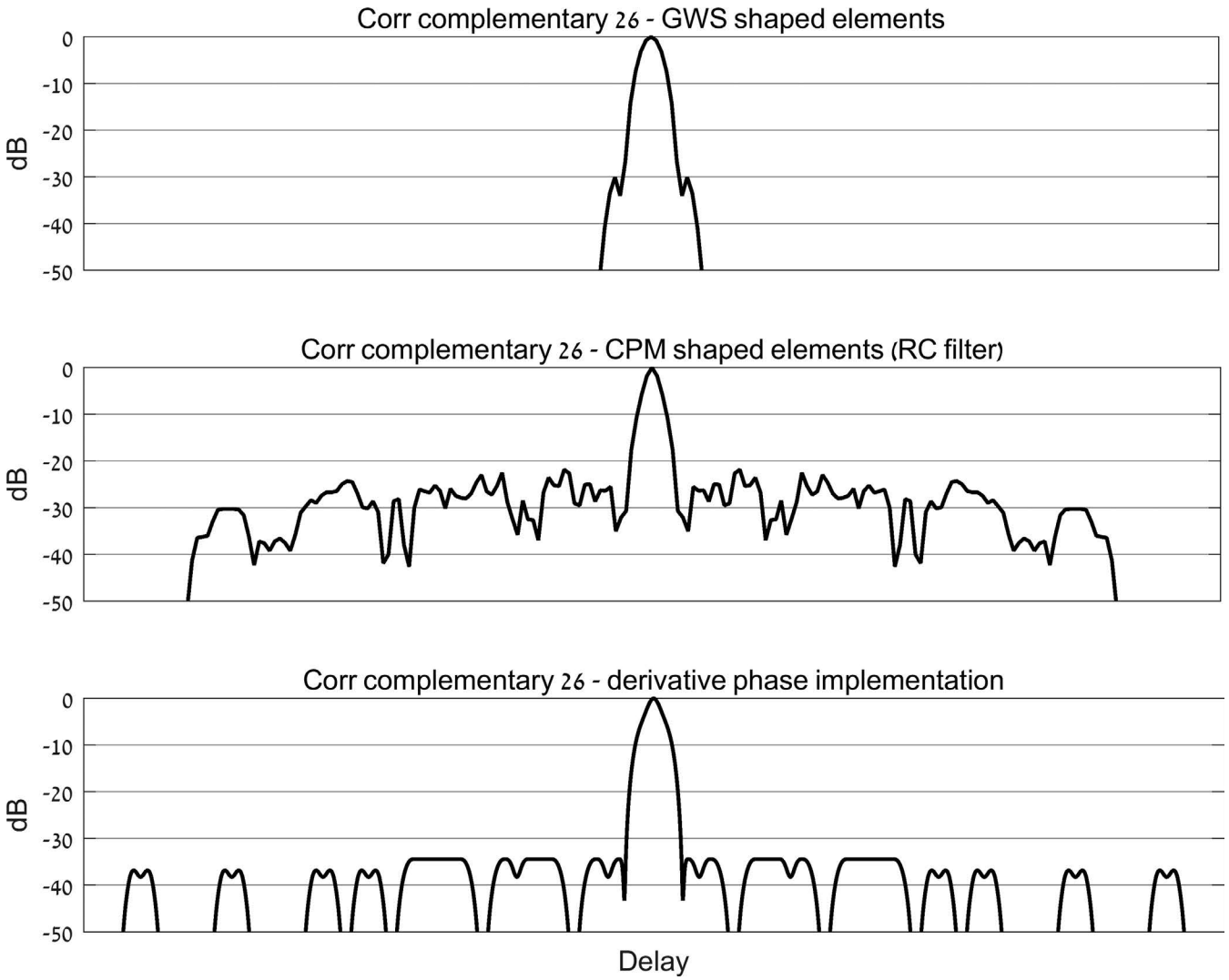

Figure 16.
ACF mainlobe comparison between three spectrally efficient implementations of a 26 element complementary pair.

riphase implementation maintains the cancellation of the ACF near-sidelobes, but the mainlobe width is doubled, with the null at $|\tau| = 2t_b$. The pulse amplitude is uniform except for the first and last bit. The spectral sidelobes decay rate is in between the rectangular bit implementation and GWS.

NEAR-SIDELOBES OF CONCATENATED COMPLEMENTARY CODES

The Doppler-induced near delay-sidelobes (see Figures 5 and 8) exhibit an interesting pattern when code pairs are created by concatenating an existing pair. The concatenating rule says that if a pair $\{[s_1]\ [s_2]\}$ is complementary then a new pair, created as $\{[s_1, s_2]\ [s_1, -s_2]\}$, will also be complementary. So will also be the pair $\{[s_2, s_1]\ [s_2, -s_1]\}$. The unique symmetry between the two codes in the new pair, combined with the Doppler generated linear phase ramp, added identically to each code in the new pair, cancel out the distant Doppler-induced near-sidelobes. This phenomenon is demonstrated in Figure 17, which used code pairs of length 52 elements each, created by concatenating the 26 element codes used so far.

In Figure 17 the floor at −65 dB was removed to expose the grid lines. It should be compared with Figures 5 and 8, where a basic kernel code of length 26 was used. In Figures 5 and 8 the near sidelobes at $\nu NT_r = 4$ and at $\nu NT_r = 68$ extend for the entire pulsewidth (= code length). In Figure 17 those sidelobes extend for only the near half of the pulsewidth. It is expected that complementary codes created by repeated concatenations will exhibit more complicated on-off sidelobe patterns.

OTHER APPROACHES

So far we have described the complementary pair's sensitivity to Doppler shift and its effect on the delay-Doppler response, as obtained with a conventional linear pulse-Doppler processor. We did not suggest any mitigation approach. However, mitigation schemes were described in the literature. In 1991

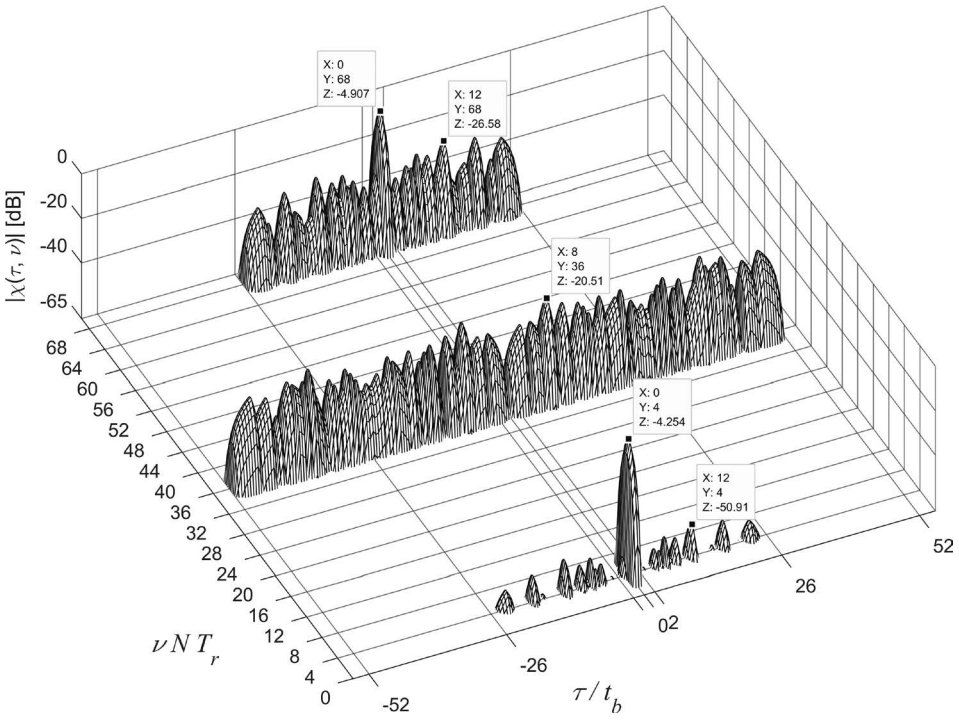

Figure 17.
Delay-Doppler response, 52 element code, Doppler shift $\nu NT_r = 4$, 2-pulse canceller, N=64 pulses. Zoom on $|\tau| \le t_p$.

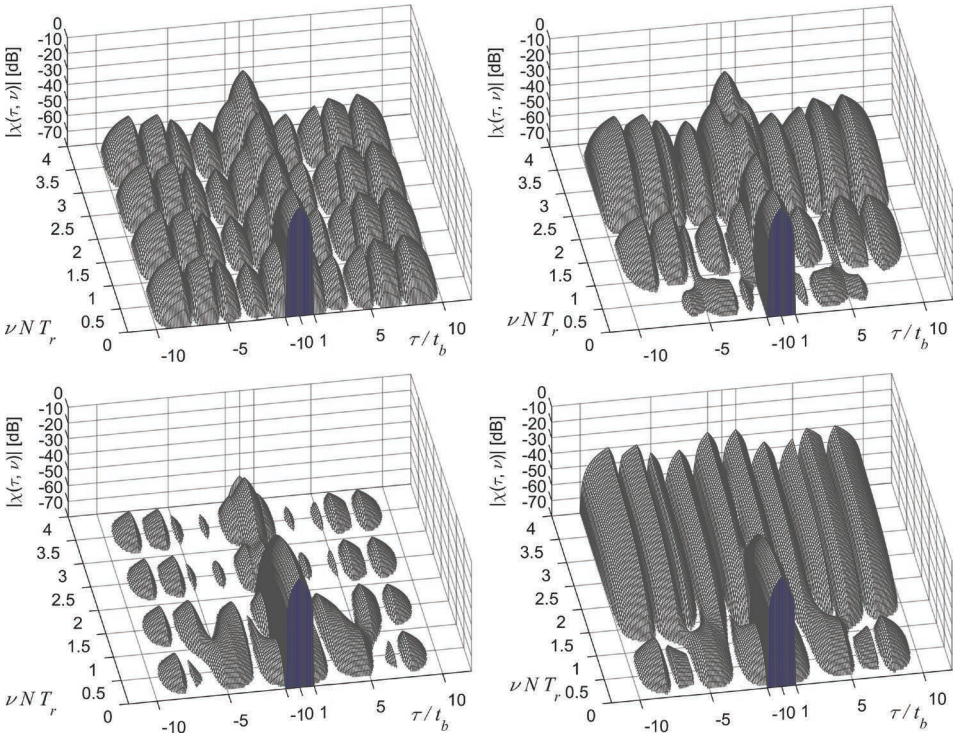

Figure 18.
Delay-Doppler response of 16 complementary pairs (32 pulses), with 10 code elements in each pulse. (Left) Conventional periodic repeats. (Right) Doppler resilient reordering. (Top) No amplitude weighting. (Bottom) Hamming amplitude weighting on receive.

B. M. Popovic [10] pointed out that the order of the sequences in a complementary set, containing more than two sequences, can significantly reduce the ambiguity function (Doppler) sidelobes.

In order to achieve useful Doppler resolution the CPI should contain many periodic repetitions of the complementary pulse pair $\{s_1\ s_2\}$. A. Pezeshki et al. [11] provided a comprehensive analysis of reordering complementary pairs to reduce Doppler induced range sidelobes. For example a Doppler resilient reordering of four pairs would be $\{s_1\ s_2\ s_2\ s_1\ s_2\ s_1\ s_1\ s_2\}$. Reference [11] also lists many related references.

In our tutorial we elected not to elaborate on the Doppler resilient reordering concept because its contribution is lost when interpulse amplitude weighting is applied on receive. This point is demonstrated in Figure 18. A ten element binary complementary code pair was used. It was either periodically repeated 16 times, for a total of 32 pulses (left side), or reordered for Doppler resilience (right side). The top row represents the delay-Doppler responses when the processor does not include interpulse amplitude weighting. In the bottom row the processor includes Hamming interpulse weighting. Without weighting the reordered sequences produced considerable sidelobe reduction at low Doppler shifts (top right). With weighting the original periodic repeat yields the best response (bottom left) in which the Doppler sidelobes remain low also at high Doppler shifts.

CONCLUSIONS

Drawbacks of complementary-pair radar waveforms were discussed and evaluated. Methods to mitigate some drawbacks were suggested. Doubling the delay in a two-pulse canceller allows applying it, as an MTI measure, to a coherent pulse train constructed from repeated binary complementary pairs. The classical presentation of the Doppler frequency response of the pulse canceller is augmented by the delay-Doppler response, which shows what happens to the range near-sidelobes at higher Doppler shifts. The emphasis in the displayed responses was on slow targets, where MTI is most needed, in order to prevent stationary clutter returns from penetrating into higher Doppler outputs through the Doppler sidelobes of the following processing stage - the weighted DFT processor. The MTI example used in the article was a two-pulse canceller. It can easily be extended to the more complex three-pulse canceller and to a modified three-pulse canceller [12].

Spectral efficiency improvement was obtained by altering the code element (bit) representation from rectangular to GWS. It was shown that the cancelling property of range near-sidelobes is maintained, but a penalty of variable amplitude is incurred. This is in contrast to constant-amplitude, spectrally efficient representations, which, however, do not maintain the perfect cancellation of the range near-sidelobes.

Recently proposed Doppler resilient reordering of binary complementary pairs, when the CPI contains many pairs, was also addressed. It was shown to underperform, compared with repetitions of the same pair, when the receiver's matched processor includes interpulse amplitude weight window. ◈

REFERENCES

[1] O'Donnell, R. M., Muehe, C. E., Labitt, M., Drury, W. H., and Cartledge, L. Advanced signal processing for airport surveillance radars. *EASCON 1974*, Washington, DC, 1974, 71A–71F.

[2] Richards, M. A. *Fundamentals of Radar Signal Processing* (2nd ed.) New York: McGraw Hill, 2014.

[3] Cook, M., Blunt, S., and Jakabosky, J. Optimization of waveform diversity and performance for pulse-agile radar. *IEEE Radar Conference*, Kansas City, MO, 2011, 812–817.

[4] Levanon, N., and Mozeson E. *Radar Signals*. New York: Wiley, 2004.

[5] Borwein, P. B., and Ferguson, R. A. A complete description of Golay pairs for length up to 100. *Mathematics of Computation*, Vol. 73, 246 (2003), 967–985.

[6] Chen, R., and Cantrell B. Highly bandlimited radar signals. *IEEE Radar Conference*, Long Beach, CA, 2002, 220–226.

[7] Faust, H. H., Connolly, B., Firestone, T. M., Chen, R. C., Cantrell, B. H., and Mokole, E. L. A spectrally clean transmitting system for solid-state phased-array radars. *IEEE Radar Conference*, Philadelphia, PA, 2004, 140–144.

[8] Blunt, S., Cook, M., Perrins, E., and de Graff, J. CPM-based radar waveform for efficiently bandlimiting a transmitted spectrum. *IEEE Radar Conference*, Pasadena, CA, 2009.

[9] Taylor, J. W., and Blinchikoff, H. J. Quadriphase code: A radar pulse compression signal with unique characteristics. *IEEE Transactions on Aerospace and Electronic Systems*, Vol. 24, 2 (1988), 156–170.

[10] Popovic, B. M. Complementary sets of chirp-like polyphase sequences. *Electronics Letters*, Vol. 27, 3 (1991), 254–255.

[11] Pezeshki, A., Calderbank, A. R., Moran, W., and Howard, S. D. Doppler resilient Golay complementary waveforms. *IEEE Transactions on Information Theory*, Vol. 54, 9 (2008), 4254–4266.

[12] Cohen, I., and Levanon, N. Adjusting 3-pulse canceller to enhance slow radar targets. *IEEE International Conference on Microwaves, Communications, Antennas and Electronic Systems (COMCAS)*, Tel Aviv, Israel, 2015.